

Cite this: *Sustainable Food Technol.*,  
2026, 4, 2129

# Optimization of maltodextrin–gum arabic–whey protein systems for freeze-drying microencapsulation of young barley leaf extract

Elham Azarpazhooh,<sup>ID</sup>\*<sup>a</sup> Yeganeh Sabeghi,<sup>ID</sup><sup>bc</sup> Masoud Najaf Najafi,<sup>\*a</sup>  
Shahin Zomorodi,<sup>d</sup> Soodabeh Einafshar,<sup>a</sup> Danial Gandomzadeh<sup>e</sup> and Xin Rui<sup>ID</sup><sup>f</sup>

Young barley leaves are rich in bioactive compounds but highly prone to oxidation, necessitating stabilization for functional food applications. This study encapsulated barley leaf extract using maltodextrin (MD), whey protein isolate (WPI), and gum arabic (GA), and optimized wall-material ratios through freeze-drying and response surface methodology (RSM). Model fitting confirmed strong statistical performance, with significant quadratic models ( $p < 0.05$ ), non-significant lack-of-fit,  $R^2$  values up to 0.99, and adequate precision above 40, ensuring reliable prediction across the design space. Experimentally, MD-rich formulations achieved the highest microencapsulation yield (~89%), while encapsulation efficiency (83.67–89.98%) maximized in a ternary MD–WPI–GA blend (67.66 : 16.67 : 16.67). Moisture content (10.22–11.29%), water activity (0.34–0.40), and particle size (34.50–37.59  $\mu\text{m}$ ) indicated good storage stability and structural integrity. Solubility reached 75.29% in MD–GA systems, and the highest glass transition temperature occurred in the ternary blend, reflecting enhanced thermal stability. Bioactive preservation was substantial, with total phenolic content (~70 mg GAE per g) and antioxidant activity (~80%) maintained effectively. Overall, MD contributed to high yield, GA to emulsion stability, and WPI to improved film-forming and antioxidant protection. The optimized microcapsules demonstrated strong stability and functional potential for use in nutraceuticals, functional foods, and instant beverage formulations.

Received 3rd December 2025  
Accepted 8th January 2026

DOI: 10.1039/d5fb00906e

rsc.li/susfoodtech

## Sustainability spotlight

This study supports sustainability in food systems by enhancing the stability of young barley leaf extract—an underutilized but nutrient-dense crop—through optimized freeze-drying microencapsulation. By preserving antioxidant and bioactive compounds without relying on synthetic additives or harsh thermal processes, the work enables the development of natural, shelf-stable ingredients for functional foods and nutraceuticals. The approach leverages readily available, food-grade wall materials (maltodextrin, gum arabic, and whey protein isolate), offering a practical and scalable strategy to reduce nutrient loss, extend product shelf life, and minimize food waste. In doing so, it contributes to sustainable innovation in food preservation and the promotion of health-supportive, plant-based products.

## 1. Introduction

Young barley leaves (*Hordeum vulgare*) have gained significant attention for their rich nutritional and bioactive composition,

<sup>a</sup>Department of Agricultural Engineering Research Department, Khorasan Razavi Agricultural and Natural Resources Research and Education Center, AREEO, Mashhad, Iran. E-mail: azarpazhooh@gmail.com; mnajafi.mhd@gmail.com

<sup>b</sup>Department of Food Science and Technology, Faculty of Agriculture, Ferdowsi University of Mashhad, Iran

<sup>c</sup>Department of Food Science and Technology, Faculty of Agriculture, Technical and Vocational University (TVU), Iran

<sup>d</sup>Agricultural Engineering Research Department, West Azerbaijan Agricultural and Natural Resources Research and Education Center, AREEO, Urmia, Iran

<sup>e</sup>Department of Mechanical Engineering, Technical and Vocational University (TVU), Iran

<sup>f</sup>College of Food Science and Technology, Nanjing Agricultural University, 14 1 Weigang Road, Nanjing 211306, China

including essential minerals, vitamins (B-complex, C, and E), chlorophyll,  $\beta$ -carotene, and antioxidant enzymes such as superoxide dismutase and catalase.<sup>1</sup> These components contribute to their well-documented physiological benefits, including antioxidant protection, immune support, lipid and glucose levels regulation, and modulation of gut microbiota.<sup>2,3</sup> Consequently, barley leaf-based powders, beverages, and nutraceutical supplements have become increasingly popular in global health-oriented food markets.<sup>4</sup>

The beneficial effects of young barley leaves are primarily attributed to phenolic acids, flavonoids such as saponarin, polysaccharides,  $\beta$ -glucans, and phytosterols.<sup>2,5</sup>

Despite these advantages, the direct use of barley leaf extract faces significant limitations due to the instability of its bioactive compounds, which are highly sensitive to environmental factors such as heat, light, oxygen, and pH.<sup>3</sup> To overcome these



challenges, microencapsulation has emerged as a powerful technique for stabilizing and protecting bioactive compounds during processing and storage.<sup>6</sup> This approach involves coating bioactive compounds with polymeric or non-polymeric materials, thereby enhancing their stability, improving sensory quality by masking undesirable flavors, and even increasing food safety through inhibition of microbial growth.<sup>6</sup> The effectiveness of encapsulation depends largely on the choice of wall material, which must provide protection, ensure controlled release, and maintain compatibility with the core compound.<sup>7</sup>

Among the various wall materials, carbohydrates (*e.g.*, maltodextrin (MD), modified starch, cyclodextrins), gums (*e.g.*, gum arabic, agar, carrageenan), lipids (*e.g.*, waxes, beeswax, diacylglycerols), and proteins (*e.g.*, casein, gelatin, whey protein isolate (WPI)) have been extensively studied.<sup>8</sup> Maltodextrin and gum arabic (GA) are particularly favored for their solubility, biocompatibility, and film-forming properties,<sup>6,9</sup> while WPI has attracted attention for its nutritional value, emulsifying ability, and capacity to stabilize hydrophobic compounds.<sup>7,10</sup> Combining these materials often enhances encapsulation efficiency and product stability, addressing the shortcomings of using each material individually.<sup>11</sup>

Among encapsulation methods, freeze-drying (lyophilization) is especially suitable for heat-sensitive bioactive compounds, as it avoids thermal degradation and preserves functional properties.<sup>10,11</sup> For instance, da Silva Júnior *et al.*<sup>12</sup> demonstrated that ciriguela peel extracts had higher quercetin and kaempferol retention in freeze-dried capsules compared with spray-dried ones. Several studies have demonstrated the successful microencapsulation of fruit and herbal extracts using maltodextrin, gum arabic, and protein-based carriers. However, most investigations have focused on single or binary wall systems, with limited systematic exploration of ternary formulations. For instance, Ledari *et al.*<sup>10</sup> encapsulated chlorophyll using maltodextrin and WPI with both freeze-drying (FD) and spray-drying (SD), reporting that FD microcapsules exhibited smaller particle sizes and higher  $\zeta$ -potential compared to SD. As well, in lipid-based nano-encapsulation, Choudhary *et al.*<sup>13</sup> reported that amorphous freeze-dried nanostructures of linseed-oil carriers, demonstrating high encapsulation efficiencies of  $84.32 \pm 1.08\%$  for LA and  $79.63 \pm 1.41\%$  for  $\beta$ -carotene.

Todorović *et al.*<sup>14</sup> encapsulated bilberry anthocyanins with maltodextrin, gum arabic, and their mixture, demonstrating that maltodextrin provided the best protection for anthocyanins during storage. Sirichokworakit *et al.*<sup>15</sup> compared different encapsulants for *Wolffia globosa* extract and found that maltodextrin combined with whey protein concentrate achieved the highest encapsulation efficiency and stability. Similarly, Ezhilarsi *et al.*<sup>16</sup> microencapsulated cowa fruit extract using WPI, MD, and their mixture, achieving high recovery of hydroxycitric acid (>85% free and >90% total) in all formulations. Despite these advances, research on ternary combinations, particularly MD–GA–WPI, remain scarce.

To date, no optimized ternary encapsulation system has been specifically developed for young barley leaf extract, despite its high susceptibility to oxidation due to abundant enzymatic

antioxidants and chlorophyll. Existing studies have mainly focused on fruit-based or by-product extracts, leaving a clear gap regarding green cereal leaf matrices with complex phytochemical profiles. Therefore, this study aimed to optimize a MD–GA–WPI system for freeze-drying microencapsulation of young barley leaf extract using response surface methodology (RSM). The innovation lied in evaluating the synergistic effects of three biopolymers on encapsulation efficiency, powder characteristics, and retention of antioxidant compounds, enabling the development of stable, bioactive-rich barley leaf powders for functional food and nutraceutical applications. Beyond technological aspects, this work also highlighted sustainability benefits, as effective encapsulation can improve resource efficiency, reduce nutritional losses, and support low-dosage delivery formats for ingredients derived from dedicated cultivation systems such as young barley leave.

## 2. Material and method

### 2.1. Materials

Young barley leaves were sourced from the Green Sprout Technology Development Company, located in the Agricultural and Natural Resources Technology and Innovation Village, Khorasan Razavi, Iran (36.30°N, 59.62°E). The crop was cultivated under commercial field conditions during the spring growing season of 2023, with irrigation following standard agronomic practices for young barley production. Leaves were harvested 18–20 days after emergence, corresponding to the early vegetative stage characterized by high chlorophyll and phenolic accumulation. Harvesting was conducted in the early morning to minimize thermal and oxidative stress and to preserve metabolite integrity. Upon arrival, the fresh leaves were washed thoroughly with distilled water to remove impurities, cut into small pieces, and dried using a hot-air dryer (Enex-Co-600; Enex, Koyang, Korea) at 70 °C for 24 h. The dried leaves were then pulverized using a blender (KA-2610; Jworld Tech, Ansan, Korea) for 30 s and passed through a 35-mesh sieve to obtain a uniform powder. The powdered samples were packed in polyethylene bags and stored at –20 °C until further use.

Maltodextrin (dextrose equivalent 20), gum arabic, and whey protein isolate were purchased from Sigma-Aldrich Co. (St. Louis, MO, USA). As well, all other chemicals and reagents used in this study were of analytical grade and obtained from Sigma-Aldrich Co. (St. Louis, MO, USA) and Merck Co. (Darmstadt, Germany).

### 2.2. Methods

#### 2.2.1. Extraction of young barley leaf bioactive compounds.

Young barley (*Hordeum vulgare* L.) leaves were sourced from a commercially cultivated crop intended specifically for the production of functional green ingredients. The raw material was provided by Green Sprout Technology Development Company, which maintains controlled cultivation practices to ensure consistent phytochemical quality. Although the leaves do not originate from agricultural residues, the dedicated



production system enables optimized resource inputs and efficient harvesting for nutraceutical applications.

Young barley leaf powder (10 g) was extracted using 100 mL of 70% (v/v) ethanol at a solid-to-solvent ratio of 1 : 10 (w/v). The mixture was kept in the dark at 25 °C for 48 h under occasional stirring to facilitate the release and solubilization of bioactive compounds. After filtration through Whatman No. 1 paper, the filtrate was concentrated under reduced pressure at 40 °C (Heidolph, Germany) and further dried in a vacuum-oven drying at 0.1 kPa (Memmert VO 400, Frankfurt, Germany) for 48 h. The dried extract was weighed to determine extraction yield and stored at −18 °C until analysis.<sup>17</sup>

**2.2.2. Preparation of microcapsules.** For the preparation of microcapsules, different proportions of maltodextrin, whey protein isolate, and gum arabic (Table 1) were dissolved in distilled water to obtain 10% (w/v) wall material solutions. The wall composition ratios used in mixture design came from a Simplex Centroid Mixture Design framework using RSM-based experimental space generation, developed in Design-Expert. The mixtures were stirred on a magnetic stirrer (400 rpm) at 35 °C for 30 min to ensure complete dissolution and then stored at 4 °C for 24 h to allow full hydration of the wall materials. After hydration, the solid dried barley leaf extract (core material) was incorporated into the wall solutions at a core-to-wall ratio of 1 : 5 (w/w). The mixture was homogenized using an Ultra-Turrax homogenizer (IKA T50, Staufen, Germany) at 12 000 rpm for 5 min, followed by sonication (Eurosonic 4D, Italy; 300 W, 50 kHz) for 1 min in an ice bath to achieve a uniform and stable solutions. The prepared solutions were then pre-frozen at −70 °C for 19 h to minimize foam formation during drying and to avoid heating of the solution due to the sonication procedure. Freeze-drying was carried out in a laboratory freeze dryer (Operon FDB-550, Seoul, Korea) at −55 °C and 0.15 mmHg for 20 h. Approximately 200 mL of each solution was freeze-dried in stainless steel. After drying, the resulting powders were gently ground with a mortar and pestle,

sieved through a 500 µm mesh (ISO 3310-ASTM E11 standard), and packed in airtight polyethylene containers under a nitrogen atmosphere to avoid oxidation. The powders were stored either at −40 °C or in the dark at room temperature (20–22 °C) until further physicochemical analyses.<sup>18</sup>

**2.2.3. Estimated encapsulation efficiency (EE) and microencapsulation yield (MY).** Encapsulation efficiency (EE) and microencapsulation yield (MY) were determined according to the method described by González-Ortega *et al.*<sup>19</sup> Encapsulation efficiency of young barley leaf extract was determined by quantifying both surface (unencapsulated) and total young barley leaf extract in the microencapsulated powders. For the estimation of surface, approximately 100 mg of powder was accurately weighed into microcentrifuge tubes, to which 1 mL of a methanol-ethanol solution (1 : 1, v/v) was added. The suspension was vortexed for 1 min to extract non-encapsulated young barley leaf extract, followed by centrifugation at 3000×g for 2 min at room temperature (Hermle Z383 K, HERMLE Labortechnik, Wehingen, Germany). The supernatant was collected, and young barley leaf extract content was analyzed spectrophotometrically. As well, total young barley leaf extract content was quantified by dissolving an equivalent amount of powder in the same solvent system, followed by extended vortexing and sonication (30 min) to ensure complete rupture of the microcapsules. After centrifugation, the young barley leaf extract concentration in the supernatant was measured under the same analytical conditions. Encapsulation efficiency (%) was then calculated using eqn (1).

$$EE(\%) = \frac{m_{\text{total}} - m_{\text{surface}}}{m_{\text{total}}} \quad (1)$$

Microencapsulation yield was determined gravimetrically and expressed as the percentage ratio between the weight of the freeze-dried microencapsulated powder ( $W_{\text{final}}$ ) and the theoretical dry weight of the wall materials used in the formulation ( $W_{\text{initial}}$ ), according to eqn (2).

$$MY(\%) = \frac{W_{\text{final}}}{W_{\text{initial}}} \times 100 \quad (2)$$

**Table 1** Wall composition based on RSM for the microencapsulation of barley leaf extract

| Run | Wall composition (%) |              |            |
|-----|----------------------|--------------|------------|
|     | Maltodextrin (20 DE) | Whey protein | Arabic gum |
| 1   | 16.67                | 16.67        | 66.67      |
| 2   | 0                    | 0            | 100        |
| 3   | 0                    | 100          | 0          |
| 4   | 0                    | 100          | 0          |
| 5   | 50                   | 50           | 0          |
| 6   | 0                    | 50           | 50         |
| 7   | 0                    | 0            | 100        |
| 8   | 50                   | 0            | 50         |
| 9   | 100                  | 0            | 0          |
| 10  | 66.67                | 16.67        | 16.67      |
| 11  | 100                  | 0            | 0          |
| 12  | 50                   | 50           | 50         |
| 13  | 33.33                | 33.33        | 33.33      |
| 14  | 16.67                | 66.67        | 16.67      |

**2.2.4. Determination of the physical properties of microcapsules.** The physical properties of the freeze-dried powders including moisture content, water activity, bulk density, and solubility index were evaluated following the method of Sharayei *et al.*<sup>20</sup> with slight modifications.

The moisture content of the freeze-dried powders was determined by gravimetric analysis. Approximately 2 g of each powder was weighed and dried in a hot air oven (Memmert, UFB 500, Schwabach, Germany) at 105 ± 1 °C until a constant weight was achieved. Results were expressed as a percentage of weight loss on a dry basis.

Water activity ( $a_w$ ) was measured at 25 °C using a dew-point-based water activity instrument (Pre AquaLab, USA).

Two grams of powder were carefully transferred into a pre-weighed 10-mL graduated cylinder without compacting. The cylinder was tapped three times on the bench to settle the



powder, and the final volume was recorded. Bulk density was calculated as the ratio of the sample mass (g) to the occupied volume (cm<sup>3</sup>) and expressed in g cm<sup>-3</sup>.

Approximately 1 g of powder was dispersed in 100 mL of distilled water and stirred using a magnetic stirrer (ARE, Velp, Italy) at 400 rpm for 5 min at 25 °C. The suspension was then centrifuged at 3000 rpm for 5 min at 25 °C using a laboratory centrifuge (Hermle Z383 K, HERMLE Labortechnik, Wehingen, Germany).

An aliquot of 20–25 mL of the supernatant was transferred to a pre-weighed glass Petri dish and dried either at 70 °C overnight or at 105 °C for 5 h until constant weight. The solubility index (%) was calculated as the ratio of the dry weight of solids recovered after drying to the initial weight of powder used, according to eqn (3).

$$\text{Solubility}(\%) = \frac{\text{weight of dried supernatant}(\text{g})}{\text{initial powder weight}(\text{g})} \times 100 \quad (3)$$

**2.2.5. Glass transition temperature determination.** The glass transition temperature ( $T_g$ ) of the microcapsule powders was determined using differential scanning calorimetry (DSC) equipped with a liquid nitrogen cooling system. The instrument was calibrated with indium and zinc standards for temperature and heat flow accuracy. Approximately 5–10 mg of sample was accurately weighed into a 50  $\mu\text{L}$  aluminum pan (hermetically sealed with pierced lids to allow evaporation of residual water) and analyzed against an empty sealed aluminum pan as reference. Samples were subjected to a heating–cooling–reheating program to remove their thermal history. Initially, powders were cooled to  $-40$  °C and equilibrated for 5 min, then heated from  $-40$  °C up to 200 °C at a rate of 10 °C min<sup>-1</sup>, equilibrated at 200 °C for 5 min, and subsequently cooled back to  $-40$  °C at 10 °C min<sup>-1</sup>.<sup>21</sup>

**2.2.6. Particle size distribution analysis.** The particle size distribution of the microcapsules was evaluated using a laser light scattering method (SAL, D-2101, Shimadzu, Japan). To prepare the sample, an appropriate amount of microcapsule powder was dispersed in hexane and subjected to sonication for approximately 2 min using an ultrasonic homogenizer (Labofuge 200, Heraeus Sepatech, Germany) to ensure uniform dispersion. The resulting suspension was immediately transferred into the measurement cell of the analyzer, and particle size data were directly recorded and processed using the instrument software (Parrarud, 2010; Pranee). Measurements were carried out at 25 °C, and all analyses were performed in triplicate. Results were reported as mean  $\pm$  standard deviation.<sup>22</sup>

**2.2.7. Microstructure analysis.** The morphology and surface microstructure of the freeze-dried microcapsules were examined using scanning electron microscopy (SEM; Leo, 1450 VP, Germany). A small amount of each powder sample was randomly mounted onto aluminum stubs using conductive carbon adhesive tape. To enhance surface conductivity and improve imaging resolution, the samples were sputter-coated with a thin conductive layer of gold–palladium ( $\approx 10$  nm) for 2 min. The coated specimens were observed under a scanning

electron microscope at accelerating voltages 15 kV and with a working distance of 9 mm.

Because freeze-dried microcapsules exhibit irregular, amorphous, and non-spherical shapes, particle size was not determined as a geometric spherical diameter. Instead, particle dimensions were quantified directly from SEM micrographs using ImageJ software. For each formulation, at least 100 particles were randomly selected across multiple fields, and the longest Feret diameter (maximum caliper distance) was used as a standardized descriptor of particle size.<sup>23</sup>

## 2.2.8. Determination of the chemical properties and antioxidative

**2.2.8.1. Total phenolic content (TPC).** The total phenolic content of the microencapsulated powders was determined using the Folin–Ciocalteu colorimetric method, with slight modifications based on Sharayei *et al.*<sup>24</sup> Briefly, 10 mg of powder was dissolved in methanol and appropriately diluted with distilled water. An aliquot of the extract was mixed with 2.5 mL of Folin–Ciocalteu reagent (previously diluted 1:10 with distilled water) and allowed to react for 3 min in the dark. Subsequently, 5 mL of sodium carbonate solution (7.5%, w/v) was added, and the mixture was made up to 50 mL with distilled water. The reaction mixture was incubated in the dark at room temperature for 60 min to allow color development (in some cases up to 24 h for complete stabilization). Absorbance was measured at 765 nm using a UV-Vis spectrophotometer (Shimadzu Co., Kyoto, Japan). A calibration curve was prepared using gallic acid standard solutions (Sigma-Aldrich, Darmstadt, Germany), and results were expressed as milligrams of gallic acid equivalents per gram of dry sample (mg GAE per g DW).

**2.2.8.2. DPPH radical scavenging activity.** The antioxidant capacity of the microcapsules was assessed using the DPPH (2,2-diphenyl-1-picrylhydrazyl) radical scavenging assay. A freshly prepared 0.006% methanolic DPPH solution was used as the radical source. One milliliter of sample solution at different concentrations was mixed with 1 mL of the DPPH solution, vortexed for uniform mixing, and incubated in the dark at room temperature for 1 h. Absorbance was measured at 512 nm against a methanol blank using a UV-Vis spectrophotometer (Shimadzu Co., Kyoto, Japan). The radical scavenging activity (RSA) was calculated as inhibition percentage using eqn (4).

$$\text{Inhibition}(\%) = \frac{A_c - A_s}{A_c} \quad (4)$$

where  $A_c$  is the absorbance of the control and  $A_s$  is the absorbance of the sample.<sup>25</sup>

**2.2.9. Experimental design and statistical analysis.** In this study, a simplex centroid mixture design was applied to evaluate the combined effects of maltodextrin (MD), gum arabic (GA), and whey protein isolate (WPI) on the physicochemical and functional properties of the microencapsulated powders. Fourteen experimental runs, including three replicates at the centroid point, were generated within the mixture space (Table 1). The proportions of MD, GA, and WPI were considered as independent variables. All experimental data were analyzed using Design-Expert® software version 11 (Stat-Ease Inc., Minneapolis, MN, USA). Analysis of variance (ANOVA) was



performed to determine the significance of the model terms, and mean comparisons were conducted using Duncan's multiple range test at a significance level of  $p < 0.05$ . To describe the relationship between the mixture components and the response variables, a polynomial mixture model was fitted to the data. The general form of the applied model was as follow:

$$Y = \beta_0 + \sum_{i=1}^2 \beta_i X_i + \sum_{i=1}^2 \beta_{ii} X_i^2 + \sum_{i < j=1}^2 \beta_{ij} X_i X_j \quad (5)$$

where  $Y$  is the predicted response,  $\beta_0$ ,  $\beta_i$ , and  $\beta_{ij}$  are the model coefficients, and  $X_i$  and  $X_j$  represent the proportions of the mixture components (MD, GA, and WPI). Model adequacy was evaluated through statistical criteria including  $p$ -values, lack-of-fit tests, and determination coefficients. Response surface plots were generated to visualize the interactive effects of mixture variables. Finally, numerical and graphical optimization procedures were conducted to determine the optimal combination of wall materials for producing powders with desirable characteristics. All data were reported as mean  $\pm$  standard deviation (SD).<sup>26</sup>

### 3. Results and discussion

#### 3.1. Model fitting

Multiple regression models, including linear and quadratic forms, were initially tested for all physicochemical and functional responses to ensure comprehensive model evaluation. The most appropriate model for each response was selected based on statistical significance, lack-of-fit analysis, goodness-of-fit parameters, and predictive ability. As shown in Table 2, the regression models applied to the microencapsulation data demonstrated strong statistical validity. Most responses were best described by quadratic models, with highly significant  $p$ -values ( $p < 0.05$ ), non-significant lack of fit, and high coefficients of determination ( $R^2$  up to 0.99). The close agreement between  $R^2$ , adjusted  $R^2$ , and predicted  $R^2$  (differences  $< 0.2$ ) confirmed that the models accurately captured the variability of each response without overfitting. Adequate precision values—many exceeding 40—indicated strong signal quality and reliable prediction capability within the experimental design space. Additionally, the low CV values reflected excellent repeatability of the measurements. Collectively, these metrics demonstrated

that the selected models were robust, precise, and suitable for predicting the physicochemical and functional properties of barley-leaf microcapsules across the tested formulation range.

#### 3.2. Powder yield of microencapsulation

As shown in Table 3, the microencapsulation yield (MY) ranged from 85.62% to 89.45%. This variation was directly related to the nature and proportion of the encapsulating agents used. When MD alone (100%) was employed, the highest yield of approximately 89% was obtained. This superior performance can be attributed to maltodextrin's excellent solubility, low viscosity, and strong drying properties, which reduce stickiness in the freeze dryer chamber and thus improve powder recovery. In addition, maltodextrin increases the glass transition temperature of the feed and forms a protective layer around droplets, thereby preventing stickiness and enhancing yield. These results are consistent with previous studies by Sarabandi *et al.*<sup>27</sup> and Goula and Adamopoulos,<sup>28</sup> who reported similar improvements when maltodextrin was used in the microencapsulation of date juice and orange concentrate, respectively. For WPI alone (100%), yields of around 86.86% were achieved.

**Table 3** Effect of type and concentration of wall material components (based on experimental design) on microencapsulation yield, microencapsulation efficiency, particle size ( $\mu\text{m}$ ) and glass transition temperature ( $^{\circ}\text{C}$ ) of young barley leaf extract

| Run | MY (%) | ME (%) | Particle size ( $\mu\text{m}$ ) | Glass transition temperature ( $^{\circ}\text{C}$ ) |
|-----|--------|--------|---------------------------------|---|
|     | 86.45  | 89.98  |                                 |   |
| 1   | 87.80  | 84.47  | 35.59                           | 74.24   |
| 2   | 86.86  | 87.05  | 37.59                           | 75.81   |
| 3   | 86.86  | 87.05  | 34.83                           | 76.53   |
| 4   | 85.91  | 85.63  | 35.01                           | 77.52   |
| 5   | 85.75  | 88.82  | 34.98                           | 76.32   |
| 6   | 87.80  | 84.47  | 34.82                           | 72.27   |
| 7   | 87.45  | 88.94  | 37.59                           | 75.89   |
| 8   | 89.45  | 83.67  | 35.49                           | 75.75   |
| 9   | 87.05  | 86.13  | 36.31                           | 75.29   |
| 10  | 89.00  | 85.81  | 35.21                           | 77.98   |
| 11  | 85.91  | 84.63  | 35.31                           | 75.29   |
| 12  | 85.82  | 87.13  | 36.00                           | 74.55   |
| 13  | 85.62  | 86.17  | 34.72                           | 74.42   |

**Table 2** Analysis of variance of the predicted models for the physicochemical and functional responses of microencapsulated young barley leaf powder

| Features                         | Model     | $p$ -Value | Lack of fit | $R^2$ | Adj $R^2$ | Pred $R^2$ | Adeq precision | Mean  | SD     | CV (%) |
|----------------------------------|-----------|------------|-------------|-------|-----------|------------|----------------|-------|--------|--------|
| Encapsulation efficiency         | Quadratic | 0.0072     | 0.19        | 0.74  | 0.65      | 0.49       | 6.57           | 86.42 | 1.14   | 1.32   |
| Microencapsulation yield         | Quadratic | <0.0001    | 0.99        | 0.99  | 0.99      | 0.97       | 48.01          | 86.98 | 0.11   | 0.13   |
| Moisture content                 | Quadratic | 0.0003     | 0.99        | 0.91  | 0.86      | 0.70       | 13.79          | 10.66 | 0.10   | 0.97   |
| Water activity                   | Quadratic | 0.02       | 0.94        | 0.90  | 0.85      | 0.68       | 12.78          | 0.35  | 0.0076 | 2.13   |
| Bulk density                     | Quadratic | 0.0088     | 0.95        | 0.84  | 0.78      | 0.56       | 9.36           | 0.21  | 0.01   | 5.98   |
| Solubility index                 | Linear    | <0.0001    | 0.57        | 0.90  | 0.88      | 0.82       | 17.82          | 72.53 | 1.00   | 1.38   |
| Glass transition temperature     | Quadratic | 0.03       | 0.13        | 0.62  | 0.46      | 0.03       | 7.95           | 75.47 | 1.00   | 1.33   |
| Particle size distribution       | Quadratic | 0.0028     | 0.98        | 0.91  | 0.85      | 0.69       | 11.91          | 35.57 | 0.37   | 1.06   |
| Total phenolic content           | Quadratic | <0.0001    | 0.99        | 0.99  | 0.98      | 0.97       | 44.39          | 62.18 | 0.41   | 0.67   |
| DPPH radical scavenging activity | Quadratic | <0.0001    | 0.99        | 0.98  | 0.98      | 0.96       | 42.13          | 76.80 | 0.2    | 0.54   |



WPI is known for its excellent emulsifying properties and strong film-forming ability, which reduce stickiness and hygroscopicity, thereby improving yield. The improvement is particularly pronounced at lower concentrations, where proteins migrate to the surface of droplets during drying and form a protein-rich film that prevents adhesion to chamber walls. Similar observations were reported by Wang *et al.*<sup>29</sup> in soy sauce powder and Shi *et al.*<sup>30</sup> in honey powder, where whey proteins increased powder yield by reducing stickiness. However, excessive WPI may reduce yield due to protein denaturation and heat sensitivity during drying. When GA alone (100%) was applied, the yield reached approximately 87.8%, which is higher than WPI but lower than maltodextrin. GA possesses natural emulsifying capacity and good film-forming properties, which contribute to higher recovery.<sup>31</sup> However, its higher viscosity compared to maltodextrin can lead to stickier particles and larger droplets during atomization. Nonetheless, increasing the concentration of GA generally led to higher yields, consistent with the findings of Karrar *et al.*<sup>32</sup> who reported improved microencapsulation efficiency when GA was used in higher proportions.

In contrast, mixtures of wall materials produced variable results. The binary blend of MD and WPI (50 : 50) resulted in a yield of 85.91%, lower than either component alone. This suggests that the expected synergistic effect did not occur, possibly due to an imbalance between carbohydrate drying behavior and protein thermal sensitivity. Likewise, WPI and GA (50 : 50) yielded 85.75%, offering no clear advantage. The blend of MD and GA (50 : 50) reached 87.45%, which is comparable to GA alone but still lower than maltodextrin's performance, likely due to increased viscosity from the gum fraction. Ternary formulations, such as equal proportions of MD, WPI, and GA (33 : 33 : 33), gave yields around 85.82%, while other three-way blends ranged between 85.6% and 87.05%. Although diversification of wall materials improved emulsion stability, it did not maximize yield. This may be explained by higher viscosity leading to delayed atomization and stickier particles, as reported by Ozdemir *et al.*<sup>33</sup>

### 3.3. Microencapsulation efficiency

Encapsulation efficiency (ME) is a critical parameter for improving any encapsulation procedure, regardless of the process or material involved.<sup>31</sup> In this study, ME of young leaf extract varied between 83.67% and 89.98% (Table 3), confirming that both the type and ratio of wall materials substantially influenced retention. These variations reflect differences in the polymer matrices formed by each wall material, which display distinct film-forming capacities and retention properties.<sup>33</sup> Furthermore, the physicochemical features of the wall and the core—such as emulsifying capacity, interfacial stability, and drying behavior—proved decisive in encapsulating sensitive bioactive compounds.<sup>18,34</sup>

The highest ME (89.98%) was obtained when MD dominated the formulation (MD 67.66%, WPI 16.67%, GA 16.67%). Maltodextrin is widely recognized as a highly soluble, low-viscosity carbohydrate with low sugar content and a colorless solution, properties that facilitate drying, increase the glass transition

temperature, and minimize stickiness, thereby forming a stable protective film.<sup>35</sup> Our findings suggested that MD performs best when complemented with protein and gum components. When GA alone (100%) was used, ME dropped to 84.47%. GA, a highly branched heteropolysaccharide with covalently bound glycoproteins, is well known for its film-forming and emulsifying abilities across a wide pH range. Its amphiphilic structure allows interactions with both hydrophilic and hydrophobic molecules, which strengthens emulsion stability through steric and thickening effects.<sup>36</sup> However, excessive viscosity at high concentrations can produce larger droplets and reduce recovery, explaining the lower efficiency when GA was used alone.

Similarly, MD alone (100%) yielded low efficiency (83.67–85.81%) because, although it enhances drying performance, the absence of emulsifying agents limits interfacial stability. In contrast, WPI alone (100%) achieved a higher ME of 87.05%, outperforming either MD or GA alone. This was attributed to WPI's strong emulsifying activity and its ability to migrate to the droplet surface during atomization, forming a viscoelastic protein-rich film that enhances structural integrity.<sup>36</sup> However, the heat sensitivity of proteins may limit their protective role when used as the sole encapsulant.

Mixed formulations revealed clear synergistic effects. A 50 : 50 blend of WPI and GA achieved 88.82%, while a 50 : 50 blend of MD and GA reached 88.94%, both significantly higher than single-component systems. Consistent with the earlier findings on MY, these results confirmed that GA contributes emulsification and coating capacity, while MD strengthens the protective matrix by reducing stickiness and supporting film formation.<sup>37</sup> Similar synergistic effects have been reported: Habib *et al.*<sup>38</sup> observed the highest ME (90.31%) with GA/WPI for astaxanthin, and Rashid *et al.*<sup>39</sup> achieved 85–96% ME for pomegranate peel extract using MD, WPI, and their blends, demonstrating the benefits of combining polysaccharides and proteins. Moreover, electrostatic interactions between WPI and GA are known to reinforce interfacial films, promoting higher encapsulation yields.<sup>40,41</sup>

In line with the previous discussion of MY, the MD + WPI combination (50 : 50) yielded only 84.63–85.63%, suggesting weaker synergy compared to formulations containing GA. This supported earlier findings by Barbosa *et al.*,<sup>42</sup> who emphasized that emulsion stability is directly correlated with higher ME, as stable emulsions prevent phase separation and surface deposition. The ternary formulation with equal proportions (33 : 33 : 33) produced 87.13%, whereas the blend dominated by maltodextrin (MD 67.66%, WPI 16.67%, GA 16.67%) provided the best result overall. This highlighted a single wall material cannot provide all necessary functionalities, while carefully designed blends exploit the strengths of each component.<sup>30</sup>

Finally, it is worth noting that emulsion viscosity and rheology play essential roles. As Ozdemir *et al.*<sup>33</sup> suggested, higher emulsion viscosity can enhance ME by reducing internal circulation and accelerating semi-permeable membrane formation. However, excessively high viscosity may decrease volatile retention by exposing encapsulates to high atomization temperatures.



### 3.4. Moisture content

Moisture is a crucial quality parameter of dried powders, as it directly influences drying efficiency, flowability, stickiness, caking tendency, and storage stability, primarily through its effect on glass transition temperature and crystallization behavior.<sup>32</sup> As shown in Fig. 1, the moisture content differed significantly among treatments ( $P < 0.05$ ), with values ranging from 10.22% to 11.29%. Although these levels were slightly higher than the <4% typically recommended for industrial dried powders,<sup>32</sup> they remained below the 10% threshold considered microbiologically safe.<sup>15</sup> In contrast, the non-encapsulated control sample showed a considerably higher moisture content of approximately  $12.8\% \pm 0.02$ , indicating its greater hygroscopicity and reduced drying stability when compared with all encapsulated formulations.<sup>43</sup>

The type and proportion of wall materials had a decisive effect on the final moisture content, consistent with previous reports.<sup>27</sup> Among treatments, the highest moisture was observed in the 100% WPI formulation (11.29%), which can be explained by the strong water-binding affinity of proteins and their rapid film formation during drying, which traps water inside the amorphous matrix.<sup>32</sup> Literature similarly reports increased moisture when WPI is present in blends (up to 4.56%) compared to MD-only powders ( $\sim 2.55\%$ ).<sup>15</sup> For example, Sarabandi *et al.*<sup>27</sup> observed higher moisture in sour cherry juice powders prepared with WPI, confirming proteins' water-retention effect. Garlic extract powders encapsulated with WPI based had higher moisture (3.77%) than GA/CH (2.06%), reflecting proteins' stronger affinity for water.<sup>43</sup>

Formulations rich in GA tended to show higher moisture contents (10.72%), likely due to its branched heteropolysaccharide structure with abundant hydrophilic groups that bind water molecules and hinder their release.<sup>44</sup> However, other studies reported contrasting outcomes depending on formulation: Kang *et al.*<sup>45</sup> and Premi and Sharma<sup>46</sup>

demonstrated that higher GA levels in GA–MD blends often reduced moisture, underscoring the complexity of carrier interactions.

### 3.5. Water activity

Water activity ( $a_w$ ) is a critical parameter reflecting the amount of free water available in food systems, directly influencing biochemical reactions, microbial growth, and product stability.<sup>47</sup> An increase in  $a_w$  accelerates deterioration reactions, thereby reducing shelf life.<sup>47</sup> In this study, the  $a_w$  of barley leaf powders ranged between 0.34 and 0.40 (Fig. 2). These values indicated acceptable stability, but still fall close to the upper threshold, reinforcing the importance of wall material selection.

The response surface and Cox plots (Fig. 2a and b) revealed that  $a_w$  decreased as the proportions of MD, GA, and WPI increased toward the central region of the triangular mixture design. Beyond this central point, however,  $a_w$  values began to rise again as all three wall materials increased simultaneously. Formulations rich in MD tended to exhibit higher  $a_w$  compared to those dominated by GA or WPI, highlighting the distinct functional properties of different wall materials.

Protein-based (WPI) carriers generally increase  $a_w$  due to their strong water-binding capacity, as reported for gurun seed oil and *Wolffia globosa* extracts.<sup>15,32</sup> By contrast, carbohydrate-dominant systems (GA + MD) consistently achieve lower  $a_w$  values. Likewise, anthocyanin-rich bilberry extracts encapsulated with MD and GA achieved  $a_w \leq 0.30$ , enhancing anthocyanin stability during storage.<sup>14</sup> Similarly, GA–MD blends have been shown to reduce  $a_w$  and improve encapsulation stability of blackberry powders.<sup>48,49</sup>

Other encapsulation studies confirmed these trends, for example, freeze-dried garlic extract encapsulated with WPI/CH or GA/CH achieved exceptionally low  $a_w$  ( $< 0.20$ ), ensuring strong microbial resistance.<sup>43</sup> Encapsulated  $\beta$ -carotene powders



Fig. 1 Effect of wall composition on moisture content: (a) response surface diagram, (b) Cox plot. A: MD (DE 20); B: WPI; C: GA.



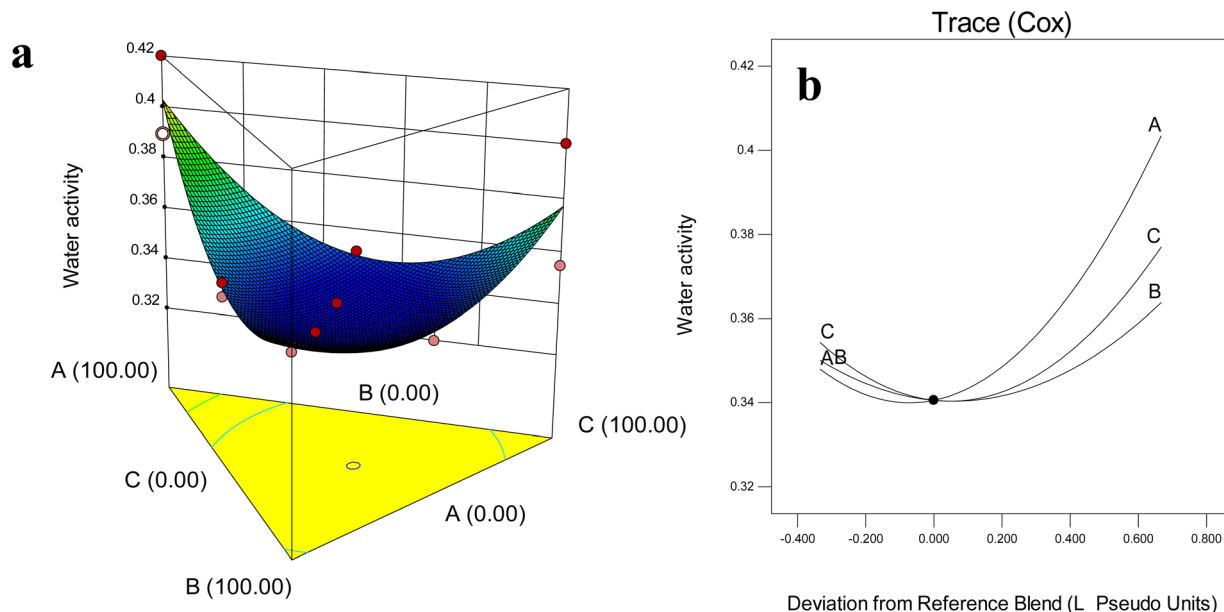


Fig. 2 Effect of wall composition on water activity: (a) response surface diagram, (b) Cox plot. A: MD (DE 20); B: WPI; C: GA.

prepared with GA or almond gum reached  $a_w$  values of 0.24–0.26, demonstrating excellent stability.<sup>50</sup> In Welsh onion juice powders,  $a_w$  values remained consistently between 0.27 and 0.37 regardless of GA:MD ratios, all below the 0.40 threshold considered safe.<sup>51</sup>

The interpretation of moisture content and  $a_w$  results demonstrated that MD can retained water in a more labile state. Conversely, WPI-containing systems exhibited higher moisture content but lower  $a_w$ , attributable to the strong water-binding properties of proteins. Therefore, the results emphasized that wall material composition governs not only total water content but also the physical state of water, with ternary MD–GA–WPI.

### 3.6. Bulk density

Bulk density is a critical property dried powders, with direct implications for transportation, storage, and packaging efficiency. It is strongly influenced by particle size, surface characteristics, and porosity; smoother, more uniform powders generally exhibit higher bulk density due to better packing ability.<sup>15</sup> In this study, the bulk density of barley leaf powders varied significantly among treatments ( $P < 0.05$ ), ranging from 0.189 to 0.276  $\text{g cm}^{-3}$  (Fig. 3a and b).

The lowest density was observed in WPI-rich formulations ( $\sim 0.18 \text{ g cm}^{-3}$ ), consistent with studies reporting that protein film formation traps air and increases porosity, creating spongy



Fig. 3 Effect of wall composition on microcapsule bulk density ( $\text{g cm}^{-3}$ ): (a) response surface diagram, (b) Cox plot. A: MD (DE 20); B: WPI; C: GA.



low-packing powders.<sup>32</sup> For instance, WPI-based encapsulation of gurun seed oil (bulk density 0.16–0.26 g cm<sup>-3</sup>), where PB (WPI:MD, 2:1) systems displayed markedly lower bulk densities compared to carbohydrate-dominant formulations.<sup>32</sup> Likewise, *W. globosa* powders encapsulated with WPI exhibited reduced density (0.15–0.16 g cm<sup>-3</sup>) compared to MD-based systems (0.32 g cm<sup>-3</sup>), reinforcing the tendency of proteins to lower packing efficiency.<sup>15</sup>

Powders with higher proportions of GA exhibited higher bulk density compared to those with MD (0.27 g cm<sup>-3</sup>). This behavior may be explained by highly branched heteropolysaccharide with covalently bound glycoproteins, which leads to improve viscosity and increased powder volume. In contrast, MD—owing to its higher excellent solubility, low viscosity—tends to occupy interstitial spaces more effectively, thereby increasing bulk density but still lower than GA-rich formulations.

### 3.7. Solubility index

Solubility is a fundamental functional property of dried powders because it determines their ability to be readily reconstituted in aqueous systems, thereby affecting the bioavailability of encapsulated compounds and their practical use in food formulations.<sup>44</sup> According to (Fig. 4a and b), the solubility results (65.00–75.29%) showed significant differences among formulations ( $P < 0.05$ ). The lowest solubility was obtained in powders prepared with the ternary combination of MD (16.67%), WPI; (66.67%), and GA (16.67%). This reduction was likely explained by proteins' high susceptibility to moisture-driven plasticization and thermal denaturation during drying, which promote protein aggregation and formation of dense, compact microstructures, limiting water permeability and delaying hydration during reconstitution.<sup>44</sup> As well, this result in lined with  $T_g$  and moisture results (refer to Sections 3.4 and 3.8), due to formulations with lower  $T_g$  values—often associated

with higher moisture—tended to demonstrate reduced solubility, particularly those with high WPI content as previously stated by Breen *et al.*<sup>52</sup>

In contrast, MD–GA blends consistently produced the highest solubility values, attributable to their highly hydrophilic nature, low viscosity, and favorable rehydration properties, making them particularly effective carriers in encapsulation processes.

Fazaeli *et al.*<sup>53</sup> showed that blackberry extract powders encapsulated with 2% MD (DE6) and 6% GA reached solubility levels as high as 87%. More recently, Sirichokworakit *et al.*<sup>15</sup> demonstrated that encapsulation of *Wolffia globosa* extract using MD alone achieved solubility up to 92.17%, whereas formulations containing GA and WPI showed reduced solubility (74.90%). Bazarria and Kumar<sup>54</sup> similarly reported that MD and GA exhibited superior solubility compared to WPI-based formulations, owing to their higher water affinity and better structural compatibility.

Furthermore, the use of encapsulating agents in combination not only influenced the solubility index but also reduced solubility time, thereby improving wettability and reconstitution properties. For instance, Sirichokworakit *et al.*<sup>15</sup> observed that MD–GA–WPI blends in encapsulated extracts exhibited shorter solubility times compared to carbohydrate-only systems, a property desirable for instant beverages and functional food products requiring rapid dissolution. Medina-Jaramillo and López-Córdoba<sup>51</sup> also reported that the addition of MD and GA improved the solubility of freeze-dried Welsh onion powders from 72% (without carriers) to 88%, highlighting their crucial role in instant food applications. Overall, for barley leaf microcapsules, the combination of MD and GA proved to be the most effective strategy for maximizing solubility, ensuring both technological functionality (instant reconstitution, stability, ease of handling) and nutritional effectiveness (enhanced delivery of bioactive compounds).



Fig. 4 Effect of wall composition on solubility index: (a) response surface diagram, (b) Cox plot. A: MD (DE 20); B: WPI; C: GA.



### 3.8. Glass transition temperatures

Differential scanning calorimetry (DSC) thermograms of all microcapsule formulations exhibited a single, clear glass transition step without detectable crystallization or additional exothermic/endothermic peaks, confirming the fully amorphous nature of the wall matrix. The absence of crystallization peaks indicated that no phase separation or ordered structural rearrangement occurred during heating, which is essential for maintaining uniform core entrapment and preventing thermally induced leakage.<sup>32</sup>

$T_g$  variations among samples were mechanistically governed by intermolecular chain interactions and plasticization effects. Our results confirmed that wall material composition plays a decisive role in determining  $T_g$ . As shown in Table 3, the microcapsules containing maltodextrin (66.67%), WPI (16.67%), and GA (16.67%) exhibited the highest  $T_g$  among all formulations tested. This suggested that these capsules maintain structural rigidity longer at ambient temperature, delaying the transition into the rubbery state and enhancing storage stability. The improved thermal resistance was likely attributed to the higher molecular weight and film-forming capacity of GA, combined with the protective glassy nature of MD, which together create a more cohesive wall structure.<sup>51</sup>

Importantly, the  $T_g$  differences observed in our formulations closely correspond to the moisture variations reported in Section 3.4. This relationship was strongly supported by Levine and Slade<sup>35</sup> identifying water as the most influential plasticizer in amorphous food systems even small increases in moisture markedly depress the  $T_g$  of synthetic and natural polymers by enhancing molecular mobility. As well, no evidence of chemical reactions (*e.g.*, oxidation, degradation, or Maillard-related thermal crosslinking) was detected during scanning, indicating that the polymer carriers remained chemically stable within the tested temperature range. This thermal behavior confirmed that release of encapsulated bioactive compounds above  $T_g$  is a diffusion-controlled physical process rather than a reaction-induced rupture or degradation event.<sup>32</sup> Comparable results have been reported in previous encapsulation studies. For example, Ozdemir *et al.*<sup>33</sup> demonstrated that basil essential oil microcapsules prepared with GA:WPI and GA:WPI:MD combinations showed significantly higher  $T_g$  values (81 °C and 71 °C, respectively) than those produced with WPI:MD alone (58.5 °C), indicating superior resistance to moisture-induced plasticization. Similarly, Karrar *et al.*<sup>32</sup> observed that GA substantially increased  $T_g$  compared to MD, due to its higher molar mass and stronger intermolecular interactions.

### 3.9. Particle size distribution and morphology

The particle size of barley leaf microcapsules, expressed as the volume-weighted mean diameter ( $D[4, 3]$ ), ranged from 34.50 and 37.59  $\mu\text{m}$  across formulations (Table 3). These values fall within the broad particle size spectrum (20–5000  $\mu\text{m}$ ) commonly reported for freeze-dried powders, where ice sublimation and structural collapse during drying typically generate heterogeneous, irregular particles.<sup>56</sup> Notably, formulations containing higher proportions of GA (100%) produced the



Fig. 5 Scanning electron microscope at different magnifications (100, 500, and 1000 $\times$  for Latin letter indices 1 to 3, respectively): (A) 50% MD and GA mixture, (B) 50% MD and WPI, (C) 100% MD, (D) 50% MD and GA mixture, (E) 100% WPI, (F) 16.66% WPI, 66.66% GA and 16.66% MD mixture, (G) 100% GA, (H) 16.66% WPI, 16.66% GA and 66.66% MD mixture, (I) 66.66% MD, 16.66% GA and 16.66% WPI mixture, (J) 33.3% MD, 33.3% GA and 33.3% WPI mixture.



largest particles (37.59  $\mu\text{m}$ ), suggesting that the high viscosity and strong emulsifying properties of GA promoted the formation of bulkier and more cohesive particles, a trend that was further reflected in their bulk density behavior. In contrast, samples rich in WPI consistently showed the smallest diameters (34.50–35.01  $\mu\text{m}$ ), a finding consistent with their strong film-forming capacity that entraps air, yielding a spongy and porous microcapsule structure.

Maltodextrin-dominated systems (100% MD or MD-rich blends) resulted in intermediate sizes (35.21–36.31  $\mu\text{m}$ ). This trend indicates that MD, with its excellent solubility, low viscosity, tended to produce looser particles. Similarly, purple corn anthocyanin powders encapsulated with MD alone displayed small and uniform particles (8–80  $\mu\text{m}$ ), whereas MD–GA and MD–WPI systems resulted in broader distributions (10–100  $\mu\text{m}$ ) because of increased polydispersity and aggregation.<sup>57</sup>

Interestingly, ternary blends such as MD : WPI : GA (33.33 : 33.33 : 33.33%) and MD : WPI : GA (16.67 : 66.67 : 16.67%) yielded the smallest average sizes (34.50–34.72  $\mu\text{m}$ ), implying a synergistic effect between protein–polysaccharide interactions that restricted particle growth.

Our results aligned with grape seed extract encapsulation trials, where binary WPC–MD and WPC–GA systems (4 : 1 or 3 : 2) produced smaller particles compared to single carriers, underscoring the stabilizing effect of polysaccharide–protein interactions.<sup>58</sup> As well, basil essential oil microcapsules exhibited much smaller sizes (0.47–4.18  $\mu\text{m}$ ), with GA and GA–protein systems forming homogeneous distributions, illustrating the influence of emulsion viscosity and stability on final size.<sup>33</sup>

The microstructure of young barley leaf powders, as examined by SEM shown in Fig. 5, clearly demonstrates the powders prepared GA based powders showed deeper surface wrinkles. This effect can be explained by the rapid formation of a proteinaceous shell during the early drying stages, which limits water diffusion across the matrix.<sup>59</sup> Increasing GA concentration further enhanced feed viscosity and film thickness, slowing down water evaporation and yielding particles with greater wrinkling.<sup>27</sup>

SEM images of the prepared microcapsules at different magnifications (50 $\times$ , 500 $\times$ , and 1000 $\times$ ) are presented in Fig. 5. The freeze-dried microcapsules lacked defined spherical shapes and instead exhibited irregular, flake-like, and porous morphologies. This is typical of freeze-dried powders, where sublimation of ice crystals under low pressure and temperature leaves behind sponge-like or plate-like aggregates.<sup>60</sup> Such irregular glassy structures, formed after milling and sieving, reflect the mechanical stress of processing. These findings were consistent with previous freeze-dried encapsulates of bilberry extract, buriti oil, and onion leaf juice, all of which exhibited broken-glass or crystalline-like morphologies.<sup>14,47,51</sup>

Notably, wall composition strongly influenced surface features. Microcapsules prepared with MD and GA showed smooth but uneven surfaces, with limited agglomeration and slight surface curvature. By contrast, capsules formed solely with GA or MD were more brittle, displaying deeper surface indentations and wrinkles. Similar trends have been observed in basil essential oil and *Wolffia globosa* extract microcapsules,

where MD produced smoother but more cracked structures, while GA caused irregular, shrunken particles with concave shapes.<sup>15,61</sup> WPI, either alone or combined with polysaccharides, consistently reduced shrinkage and surface cracking, producing smoother morphologies due to its greater film-forming ability and flexibility during drying.<sup>15,32</sup> These smoother structures were particularly relevant, as they were associated with improved encapsulation efficiency and better retention of bioactive compounds.

Such variability highlights the importance of tailoring encapsulation systems: while MD provides good solubility and smooth surfaces, its high hygroscopicity may lead to stickiness at higher loads.<sup>14</sup> GA ensures emulsion stability and smaller particle sizes but introduces greater shrinkage, whereas WPI imparts flexibility and stability to the capsule wall, minimizing cracks and enhancing structural cohesiveness.

### 3.10. Total phenolic content and antioxidant activity

The total phenolic content (TPC) of the barley leaf microcapsules ranged from 57.11 to 69.97  $\text{mg g}^{-1}$  (Fig. 6a and b). Although the numerical range appears moderate, the differences among formulations were statistically significant ( $p < 0.05$ ), and the quadratic model demonstrated excellent predictive performance ( $R^2 = 0.99$ ;  $\text{Pred-}R^2 = 0.97$ ; Table 2), confirming that wall material composition exerted a meaningful influence on phenolic retention. Among the tested formulations, the microcapsules prepared with a 50 : 50 blend of MD and GA exhibited the highest phenolic retention, while those containing 100% GA showed the lowest levels. In contrast, the non-encapsulated control sample showed a markedly lower estimated TPC of approximately  $50 \text{ mg g}^{-1} \pm 0.17$ . This outcome confirmed that wall material composition plays a decisive role in determining the efficiency of phenolic preservation during drying. Previous studies also highlighted that wall–core interactions, the volatility of encapsulated compounds, and the molecular size and flexibility of wall materials strongly affect the diffusion of phenolics through the capsule wall, and thus their stability.<sup>15</sup>

The Cox response plots (Fig. 6) demonstrated that TPC initially increased with rising MD concentration up to 33.33%, but declined thereafter. A similar trend was observed in MD–GA combinations, suggesting an optimal carrier ratio for maximizing phenolic retention. These findings were consistent with earlier reports showing that MD with DE 20 provides superior oxygen barrier properties, which reduce oxidative degradation and favor the entrapment of sensitive polyphenols.<sup>6,62</sup> This protective capacity is complemented by its high solubility and low viscosity, enabling MD to more effectively occupy interstitial spaces and decrease bulk density, thereby enhancing the structural compactness and stability of the powders.<sup>15,61</sup> Comparable observations were made in bilberry and grape seed extract studies, where MD-based carriers provided higher TPC protection than GA alone.<sup>14,58</sup>

The DPPH radical scavenging activity also differed significantly across formulations ( $p < 0.05$ ; Fig. 6c and d), supported by strong model statistics ( $R^2 = 0.98$ ;  $\text{Pred-}R^2 = 0.96$ ; Table 2). The





Fig. 6 Effect of wall material composition on (a) phenolic content (mg gallic acid per g DW) illustrated by the response surface diagram and (b) Cox plot, and free radical scavenging activity (DPPH, %) shown in (c) response surface diagram and (d) Cox plot. Wall components: A: MD (DE 20); B: WPI; C: GA.

highest radical scavenging activity was observed in ternary formulations containing MD (66.67%), WPI (16.67%), and GA (16.67%), while the lowest was detected in capsules made of equal proportions of WPI and GA and the control ( $60\% \pm 0.22$ ). The MD–WPI blend also produced comparatively low activity, although its values were slightly higher than those of WPI–GA. Cox response plots (Fig. 6d) also indicated that radical scavenging activity increased with MD up to 66.67% and then decreased, while higher proportions of GA and WPI contributed positively within moderate levels. The synergistic effect of MD's protective film-forming capacity, GA's stabilizing and emulsifying properties, and WPI's inherent antioxidant activity through sulfhydryl groups has also been highlighted in studies on beetroot and mulberry polyphenol encapsulation.<sup>61,63</sup> As well these results aligned with prior work on mulberry juice and

purple corn anthocyanins, where MD–GA systems outperformed single-carrier or protein-dominant systems in stabilizing phenolic compounds during drying.<sup>57</sup> Additionally, WPI incorporation was found to enhance antioxidant performance, consistent with reports that moderate protein fractions improve phenolic entrapment and bioactivity.<sup>46,58</sup> Generally, these results confirmed that MD provided excellent oxygen resistance and solubility, GA enhanced stability and film strength, and WPI contributed functional antioxidant activity. This structural synergy not only protects phenolic compounds during freeze drying but also improves their release and functional performance upon rehydration, making these formulations particularly promising for use in functional foods and nutraceutical powders.



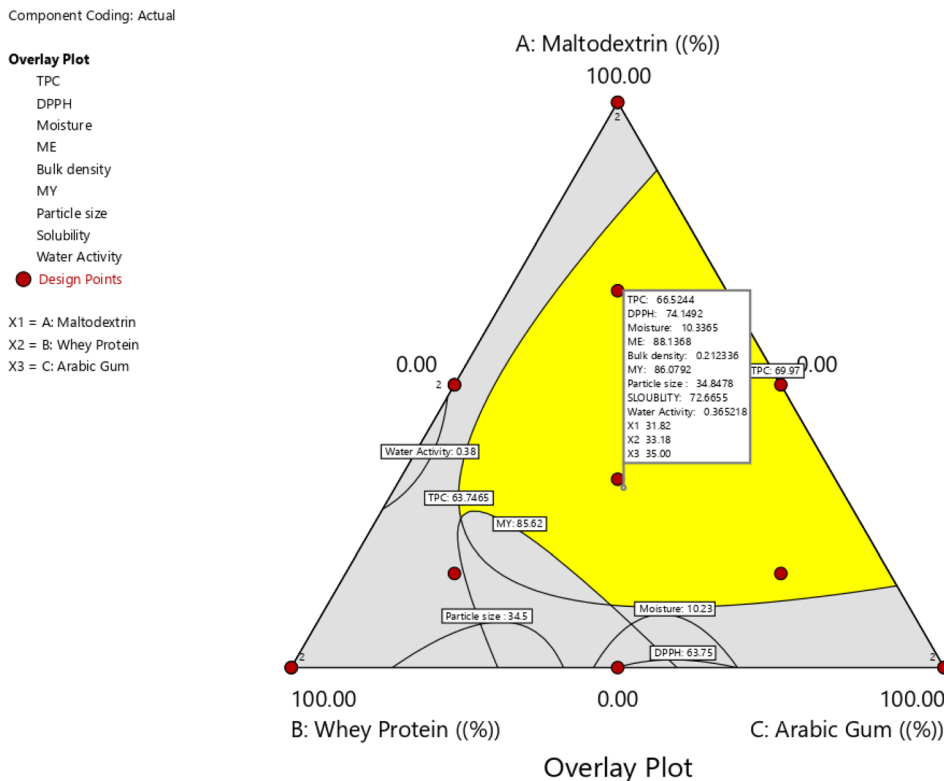


Fig. 7 Ternary overlay plot of formulations containing MD (A), WPI (B), and GA (C) in percentage (%). The yellow area shows the optimal mixture region meeting key physicochemical criteria, while red points represent tested experimental formulations with corresponding response contours.

### 3.11. Optimization

The optimal concentrations of wall materials for the microencapsulation of young barley leaf extract were determined using both numerical and graphical optimization. The graphical optimization results supporting the selection of the optimal wall material ratios are presented in Fig. 7.

The primary objectives were to maximize MY and EE, while simultaneously maintaining favorable physicochemical and functional properties. The desirability function identified an optimal wall composition of 31.81% MD, 35.00% GA, and 33.18% WPI.

Although the numerical differences among the tested formulations were moderate, the statistical Quadratic models used for optimization demonstrated strong predictive performance for key responses (MY:  $R^2 = 0.99$ ; EE:  $R^2 = 0.74$ ; moisture content:  $R^2 = 0.91$ ; TPC:  $R^2 = 0.99$ ; DPPH activity:  $R^2 = 0.98$ ; Table 2). These diagnostics indicated that even modest shifts in wall material ratios produced statistically meaningful effects—

especially for responses most relevant to microencapsulation stability and efficiency.

To ensure reproducibility and optimization robustness, the predicted optimal formulation was experimentally validated by preparing three fully independent microcapsule production batches ( $n = 3$ ).

Under the optimized conditions, the microcapsules achieved a production yield of 86.08%, encapsulation efficiency of 88.13%, TPC of  $66.52 \text{ mg g}^{-1}$ , and radical scavenging activity of 74.15%. Moisture content ( $10.37\%$ ) and bulk density ( $0.21 \text{ g cm}^{-3}$ ) also remained within desirable ranges, supporting powder stability.

To ensure robustness, the optimal formulation was experimentally validated. Independent experiments conducted at the predicted optimal ratios produced results that were statistically indistinguishable from model predictions ( $p > 0.05$ ), as shown in Table 4. This agreement confirmed that the optimization procedure was reliable and that the selected formulation

Table 4 Effect of microencapsulation with optimal wall composition (response surface methodology and experimental results) on the physical and chemical properties of microcapsule<sup>a</sup>

| Results | MY (%)                    | ME (%)                   | TPC ( $\text{mg g}^{-1}$ ) | Moisture (%)              | Bulk density ( $\text{g cm}^{-3}$ ) |
|---------|---------------------------|--------------------------|----------------------------|---------------------------|-------------------------------------|
| RSM     | 86.08 <sup>a</sup>        | 88.13 <sup>a</sup>       | 66.52 <sup>a</sup>         | 10.37 <sup>a</sup>        | 0.21 <sup>a</sup>                   |
| Test    | 84.06 ± 0.09 <sup>a</sup> | 0.01 <sup>a</sup> ± 87.5 | 0.24 <sup>a</sup> ± 67.3   | 1.05 <sup>a</sup> ± 10.30 | 1.05 <sup>a</sup> ± 0.23            |

<sup>a</sup> Values with the same letters within each column (mean ± standard deviation) are not significantly different according to Duncan's multiple range test ( $p < 0.05$ ).



provides a consistent and effective matrix for protecting the bioactive compounds in young barley leaf extract.

## 4. Conclusion

This study demonstrated that the choice and proportion of wall materials play a decisive role in determining the physico-chemical and functional properties of young barley leaf microcapsules. MD consistently enhanced powder yield, glass transition temperature, and solubility due to its favorable drying behavior, oxygen barrier capacity, and structural compactness. GA, with its strong emulsifying and film-forming capacity, improved emulsion stability and bulk density, though its higher viscosity limited yield at elevated levels. WPI contributed superior emulsification and film formation, while also enhancing antioxidant activity, but its heat sensitivity and strong water-binding capacity tended to increase moisture content and reduce bulk density.

Synergistic effects were most evident in blended systems, particularly the ternary formulation dominated by MD with moderate proportions of GA and WPI, which achieved the highest encapsulation efficiency (89.98%) and antioxidant activity (80.39%). Optimization further confirmed that a composition of 31.81% MD, 35.00% GA, and 33.18% WPI provided the most desirable balance of yield, efficiency, phenolic retention, and stability.

From an industrial perspective, the optimized microencapsulated barley leaf powder makes it suitable for incorporation into instant drink mixes, fortified bakery items, smoothies, dairy beverages, capsule supplements, and powdered nutraceutical blends. On the other hand, as young barley leaves require dedicated cultivation rather than utilizing agricultural residues, enhancing their stability and reducing nutrient loss through optimized microencapsulation supports more resource-efficient use of this high-value biomass. Future research should evaluate industrial scalability, long-term storage stability, digestive bioavailability, and integration with more sustainable drying technologies or circular-bioprocessing strategies to further strengthen economic and environmental viability.

## Conflicts of interest

There are no conflicts to declare.

## Data availability

All data generated or analyzed during this study are included in this published article. Also, more information is available from the corresponding author on request.

## Acknowledgements

We would like to express our sincere gratitude to Green Sprout Technology Development Company, for all the support related to our research.

## References

- 1 E. Kato, A. Tsuruma, A. Amishima and H. Satoh, Proteinous pancreatic lipase inhibitor is responsible for the antiobesity effect of young barley (*Hordeum vulgare* L.) leaf extract, *Biosci. Biotechnol. Biochem.*, 2021, **85**(8), 1885–1889.
- 2 M. K. Lemieszek, I. Komaniecka, M. Chojnacki, A. Choma and W. Rzeski, Immunomodulatory properties of polysaccharide-rich young green barley (*Hordeum vulgare*) extract and its structural characterization, *Molecules*, 2022, **27**(5), 1742.
- 3 K. J. Gromkowska-Kępką, R. Markiewicz-Żukowska, P. Nowakowski, S. K. Naliwajko, J. Moskwa, A. Puścion-Jakubik, *et al.*, Chemical composition and protective effect of young barley (*Hordeum vulgare* L.) dietary supplements extracts on UV-Treated human skin fibroblasts in in vitro studies, *Antioxidants*, 2021, **10**(9), 1402.
- 4 M. Wang, C. Zhang, Y. Xu, M. Ma, T. Yao and Z. Sui, Impact of six extraction methods on molecular composition and antioxidant activity of polysaccharides from young hullless barley leaves, *Foods*, 2023, **12**(18), 3381.
- 5 M. Kozłowska, M. Ziarno, D. Zaręba and I. Ścibisz, Exploring the possibility of enriching fermented milks with young barley leaves powder preparation, *Fermentation*, 2023, **9**(8), 731.
- 6 K. Sarabandi, S. M. Jafari, A. S. Mahoonak and A. Mohammadi, Application of gum Arabic and maltodextrin for encapsulation of eggplant peel extract as a natural antioxidant and color source, *Int. J. Biol. Macromol.*, 2019, **140**, 59–68.
- 7 C. Drosou and M. Krokida, A comparative study of encapsulation of  $\beta$ -carotene via spray-drying and freeze-drying techniques using pullulan and whey protein isolate as wall material, *Foods*, 2024, **13**(12), 1933.
- 8 K. Papoutsis, J. B. Golding, Q. Vuong, P. Pristijono, C. E. Stathopoulos, C. J. Scarlett, *et al.*, Encapsulation of citrus by-product extracts by spray-drying and freeze-drying using combinations of maltodextrin with soybean protein and  $\iota$ -carrageenan, *Foods*, 2018, **7**(7), 115.
- 9 L. F. Ballesteros, M. J. Ramirez, C. E. Orrego, J. A. Teixeira and S. I. Mussatto, Encapsulation of antioxidant phenolic compounds extracted from spent coffee grounds by freeze-drying and spray-drying using different coating materials, *Food Chem.*, 2017, **237**, 623–631.
- 10 S. A. Ledari, J. M. Milani, S.-A. Shahidi and A. Golkar, Comparative analysis of freeze drying and spray drying methods for encapsulation of chlorophyll with maltodextrin and whey protein isolate, *Food Chem.: X*, 2024, **21**, 101156.
- 11 L. Pudziuvelyte, M. Marksa, K. Sosnowska, K. Winnicka, R. Morkuniene and J. Bernatoniene, Freeze-drying technique for microencapsulation of *Elsholtzia ciliata* ethanolic extract using different coating materials, *Molecules*, 2020, **25**(9), 2237.
- 12 M. E. da Silva Júnior, M. V. R. L. Araújo, A. C. S. Martins, M. dos Santos Lima, F. L. H. Da Silva, A. Converti, *et al.*,



- Microencapsulation by spray-drying and freeze-drying of extract of phenolic compounds obtained from ciriguela peel, *Sci. Rep.*, 2023, **13**(1), 15222.
- 13 P. Choudhary, S. Dutta, J. Moses and C. Anandharamakrishnan, Recent developments in encapsulation of  $\alpha$ -lipoic acid for enhanced bioavailability and stability, *Qual. Assur. Saf. Crop Foods*, 2023, **15**(1), 123–138.
  - 14 A. Todorović, L. Šturm, A. Salević-Jelić, S. Lević, I. G. Osojnik Črnivec, I. Prislán, *et al.*, Encapsulation of bilberry extract with maltodextrin and gum arabic by freeze-drying: Formulation, characterisation, and storage stability, *Processes*, 2022, **10**(10), 1991.
  - 15 S. Sirichokworrakit, N. Aukkanit and C. Sangsuwon, Optimizing Encapsulation Strategies for Enhanced Antioxidant Stability of *Wolffia globosa* Extracts: A Comparative Study of Maltodextrin, Gum Arabic, and Whey Protein Concentrate, *Appl. Food Res.*, 2025, 101030.
  - 16 P. Ezhilarasi, D. Indrani, B. S. Jena and C. Anandharamakrishnan, Freeze drying technique for microencapsulation of *Garcinia* fruit extract and its effect on bread quality, *J. Food Eng.*, 2013, **117**(4), 513–520.
  - 17 S. Einafshar, A. Rohani, Y. Sabeghi, M. H. Tavassoli-Kafrani, R. Farhoosh and D. Gandomzadeh, Unveiling the power of bene (*Pistacia atlantica*) hull scum: Boosting oxidative stability with methanolic extract and ferrous ions, *Food Chem.*, 2025, **466**, 142142.
  - 18 P. Sharayei, A. Rohani, Y. Sabeghi and D. Gandomzadeh, The impact of drying techniques on stabilizing microencapsulated astaxanthin from shrimp shells: A comparative study of spray drying versus freeze drying, *J. Food Process Eng.*, 2024, **47**(11), e14755.
  - 19 R. González-Ortega, M. Faieta, C. D. Di Mattia, L. Valbonetti and P. Pittia, Microencapsulation of olive leaf extract by freeze-drying: Effect of carrier composition on process efficiency and technological properties of the powders, *J. Food Eng.*, 2020, **285**, 110089.
  - 20 P. Sharayei, E. Azarpazhooh, S. Einafshar, S. Zomorodi, F. Zare and H. S. Ramaswamy, Optimization of wall materials for astaxanthin powder production from shrimp shell extract using simplex lattice mixture design, *J. Food Process. Preserv.*, 2024, **2024**(1), 9794290.
  - 21 E. Azarpazhooh, P. Sharayei, X. Rui, M. Gharibi-Tehrani and H. S. Ramaswamy, Optimization of wall material of freeze-dried high-bioactive microcapsules with yellow onion rejects using simplex centroid mixture design approach based on whey protein isolate, pectin, and sodium caseinate as incorporated variables, *Molecules*, 2022, **27**(23), 8509.
  - 22 E. Azarpazhooh, P. Sharayei, S. Zomorodi and H. S. Ramaswamy, Physicochemical and phytochemical characterization and storage stability of freeze-dried encapsulated pomegranate peel anthocyanin and in vitro evaluation of its antioxidant activity, *Food Bioprocess Technol.*, 2019, **12**(2), 199–210.
  - 23 S. Einafshar, B. Tajeddin, Y. Sabeghi and D. Gandomzadeh, Optimization of Biodegradable Potato Starch–Nanocellulose Films: Influence of Starch Content, Nanocellulose Concentration, and Plasticizer Type, *Starch/Stärke*, 2025, e70112.
  - 24 P. Sharayei, R. Niazmand, M. S. Jamab, Y. Sabeghi, S. Einafshar, E. Azarpazhooh, *et al.*, Bioactive films from saffron corm and corn husk: A transformative solution for antioxidant and antimicrobial pistachio packaging, *LWT-Food Sci. Technol.*, 2025, 118097.
  - 25 Y. Sabeghi, M. Varidi and M. Nooshkam, Bioactive foamulsion gels: a unique structure prepared with gellan gum and *Acanthophyllum glandulosum* extract, *J. Sci. Food Agric.*, 2024, **104**(7), 3853–3864.
  - 26 E. Azarpazhooh, P. Sharayei, Y. Sabeghi, F. Zare, X. Rui and H. S. Ramaswamy, Modified atmosphere packaging of sunflower microgreens (*Helianthus annuus*) for quality and postharvest shelf-life extension, *Sustainable Food Technol.*, 2026, **15**, 2524–2535.
  - 27 K. Sarabandi, S. H. Peighambari, A. S. Mahoonak and S. P. Samaei, Effect of carrier types and compositions on the production yield, microstructure and physical characteristics of spray dried sour cherry juice concentrate, *J. Food Meas. Char.*, 2017, **11**(4), 1602–1612.
  - 28 A. M. Goula and K. G. Adamopoulos, Effect of maltodextrin addition during spray drying of tomato pulp in dehumidified air: II. Powder properties, *Dry. Technol.*, 2008, **26**(6), 726–737.
  - 29 W. Wang, Y. Jiang and W. Zhou, Characteristics of soy sauce powders spray-dried using dairy whey proteins and maltodextrins as drying aids, *J. Food Eng.*, 2013, **119**(4), 724–730.
  - 30 Q. Shi, Z. Fang and B. Bhandari, Effect of addition of whey protein isolate on spray-drying behavior of honey with maltodextrin as a carrier material, *Dry. Technol.*, 2013, **31**(13–14), 1681–1692.
  - 31 A. A. Mahdi, J. K. Mohammed, W. Al-Ansi, A. D. Ghaleb, Q. A. Al-Maqtari, M. Ma, *et al.*, Microencapsulation of fingered citron extract with gum arabic, modified starch, whey protein, and maltodextrin using spray drying, *Int. J. Biol. Macromol.*, 2020, **152**, 1125–1134.
  - 32 E. Karrar, A. A. Mahdi, S. Sheth, I. A. M. Ahmed, M. F. Manzoor, W. Wei, *et al.*, Effect of maltodextrin combination with gum arabic and whey protein isolate on the microencapsulation of gorum seed oil using a spray-drying method, *Int. J. Biol. Macromol.*, 2021, **171**, 208–216.
  - 33 N. Ozdemir, A. Bayrak, T. Tat, F. Altay, M. Kiralan and A. Kurt, Microencapsulation of basil essential oil: Utilization of gum arabic/whey protein isolate/maltodextrin combinations for encapsulation efficiency and in vitro release, *J. Food Meas. Char.*, 2021, **15**(2), 1865–1876.
  - 34 D. Gandomzadeh, M. H. Saeidirad, Y. Sabeghi, A. Rohani, E. Azarpazhooh, Y. Saeidirad, *et al.*, A comprehensive review of drying techniques and quality for saffron, *J. Food Meas. Char.*, 2024, **18**(10), 8218–8232.
  - 35 P. Sharayei, E. Azarpazhooh, F. Zare and Y. Sabeghi, Analysis of the preservation of the antioxidant, antimicrobial, and sensory capacity of free and microencapsulated shrimp



- shell extract applied in chicken lunch meat, *Translat. Food Sci.*, 2025, **1**(1), vxaf006.
- 36 S. Meena, W. Prasad, K. Khamrui, S. Mandal and S. Bhat, Preparation of spray-dried curcumin microcapsules using a blend of whey protein with maltodextrin and gum arabica and its in-vitro digestibility evaluation, *Food Biosci.*, 2021, **41**, 100990.
- 37 A. Rezvankhah, Z. Emam-Djomeh, M. Safari, M. Salami and G. Askari, Investigating the effects of maltodextrin, gum arabic, and whey protein concentrate on the microencapsulation efficiency and oxidation stability of hemp seed oil, *J. Food Process. Preserv.*, 2022, **46**(6), e16554.
- 38 S. Habib, S. M. Wani, K. Rasool, B. Ashaq, N. Anjum, S. A. Padder, *et al.*, Nanoencapsulation of astaxanthin using gum arabic and whey protein isolate as wall materials: Characterization and invitro release kinetics, *Powder Technol.*, 2025, **458**, 120982.
- 39 R. Rashid, S. M. Wani, S. Manzoor, F. Masoodi and A. Altaf, Nanoencapsulation of pomegranate peel extract using maltodextrin and whey protein isolate. Characterisation, release behaviour and antioxidant potential during simulated invitro digestion, *Food Biosci.*, 2022, **50**, 102135.
- 40 A. Bassijeh, S. Ansari and S. M. H. Hosseini, Astaxanthin encapsulation in multilayer emulsions stabilized by complex coacervates of whey protein isolate and Persian gum and its use as a natural colorant in a model beverage, *Food Res. Int.*, 2020, **137**, 109689.
- 41 A. M. Cabrales-González, D. M. Núñez-Ramírez, M. A. Martínez-Prado, L. Medina-Torres, W. Rosas-Flores and O. Manero, Microencapsulation of Acidithiobacillus thiooxidans in a biopolymeric matrix of gum arabic and whey protein using complex coacervation and freeze drying, *Miner. Eng.*, 2025, **222**, 109164.
- 42 M. Barbosa, C. Borsarelli and A. Mercadante, Light stability of spray-dried bixin encapsulated with different edible polysaccharide preparations, *Food Res. Int.*, 2005, **38**(8–9), 989–994.
- 43 L. Tavares, H. L. B. Barros, J. C. P. Vagheti and C. P. Z. Noreña, Microencapsulation of garlic extract by complex coacervation using whey protein isolate/chitosan and gum arabic/chitosan as wall materials: Influence of anionic biopolymers on the physicochemical and structural properties of microparticles, *Food Bioprocess Technol.*, 2019, **12**(12), 2093–2106.
- 44 S. Meena, S. Gote, W. Prasad and K. Khamrui, Storage stability of spray dried curcumin encapsulate prepared using a blend of whey protein, maltodextrin, and gum Arabic, *J. Food Process. Preserv.*, 2021, **45**(5), e15472.
- 45 Y.-R. Kang, Y.-K. Lee, Y. J. Kim and Y. H. Chang, Characterization and storage stability of chlorophylls microencapsulated in different combination of gum Arabic and maltodextrin, *Food Chem.*, 2019, **272**, 337–346.
- 46 M. Premi and H. Sharma, Effect of different combinations of maltodextrin, gum arabic and whey protein concentrate on the encapsulation behavior and oxidative stability of spray dried drumstick (*Moringa oleifera*) oil, *Int. J. Biol. Macromol.*, 2017, **105**, 1232–1240.
- 47 J. P. de Oliveira, O. P. Almeida, P. H. Campelo, G. Carneiro, LdO. F. Rocha, J. H. Santos, *et al.*, Tailoring the physicochemical properties of freeze-dried buriti oil microparticles by combining inulin and gum Arabic as encapsulation agents, *Lwt*, 2022, **161**, 113372.
- 48 R. V. Tonon, C. Brabet and M. D. Hubinger, Anthocyanin stability and antioxidant activity of spray-dried açai (*Euterpe oleracea* Mart.) juice produced with different carrier agents, *Food Res. Int.*, 2010, **43**(3), 907–914.
- 49 C. C. Ferrari, S. P. Marconi Germer, I. D. Alvim and J. M. de Aguirre, Storage stability of spray-dried blackberry powder produced with maltodextrin or gum arabic, *Dry. Technol.*, 2013, **31**(4), 470–478.
- 50 N. Mahfoudhi and S. Hamdi, Kinetic degradation and storage stability of  $\beta$ -carotene encapsulated by freeze-drying using almond gum and gum Arabic as wall materials, *J. Food Process. Preserv.*, 2015, **39**(6), 896–906.
- 51 C. Medina-Jaramillo and A. López-Córdoba, Enhancing the Physicochemical, Thermal, and Technological Properties of Freeze-Dried Welsh Onion Leaf Juice: Influence of Maltodextrin and Gum Arabic as Carrier Agents, *Polymers*, 2025, **17**(6), 801.
- 52 E. Breen, J. Curley, D. Overcashier, C. Hsu and S. Shire, Effect of moisture on the stability of a lyophilized humanized monoclonal antibody formulation, *Pharm. Res.*, 2001, **18**(9), 1345–1353.
- 53 M. Fazaeli, Z. Emam-Djomeh, A. K. Ashtari and M. Omid, Effect of spray drying conditions and feed composition on the physical properties of black mulberry juice powder, *Food Bioprod. Process.*, 2012, **90**(4), 667–675.
- 54 B. Bazarria and P. Kumar, Optimization of spray drying parameters for beetroot juice powder using response surface methodology (RSM), *J. Saudi Soc. Agric. Sci.*, 2018, **17**(4), 408–415.
- 55 H. Levine and L. Slade, Water as a plasticizer: physicochemical aspects of low-moisture polymeric systems, *Water Sci. Rev.*, 1988, **3**(1), 79–185.
- 56 N. J. Zuidam and E. Shimoni, Overview of microencapsulates for use in food products or processes and methods to make them, *Encapsulation Technologies for Active Food Ingredients and Food Processing*, Springer, 2009, pp. 3–29.
- 57 W. Deng, X. Li, G. Ren, Q. Bu, Y. Ruan, Y. Feng, *et al.*, Stability of purple corn anthocyanin encapsulated by maltodextrin, and its combinations with gum arabic and whey protein isolate, *Foods*, 2023, **12**(12), 2393.
- 58 K. Yadav, R. K. Bajaj, S. Mandal and B. Mann, Encapsulation of grape seed extract phenolics using whey protein concentrate, maltodextrin and gum arabica blends, *J. Food Sci. Technol.*, 2020, **57**(2), 426–434.
- 59 R. V. Tonon, C. Brabet and M. D. Hubinger, Influence of process conditions on the physicochemical properties of açai (*Euterpe oleracea* Mart.) powder produced by spray drying, *J. Food Eng.*, 2008, **88**(3), 411–418.
- 60 C. Luo, Z. Liu, S. Mi and L. Li, Quantitative investigation on the effects of ice crystal size on freeze-drying: The primary drying step, *Dry. Technol.*, 2022, **40**(2), 446–458.



- 61 S. Yousefi, M. Kavyanirad, M. Aminifar, W. Weisany and A. Mousavi Khaneghah, Yogurt fortification by microencapsulation of beetroot extract (*Beta vulgaris* L.) using maltodextrin, gum arabic, and whey protein isolate, *Food Sci. Nutr.*, 2022, **10**(6), 1875–1887.
- 62 S. A. Mahdavi, S. M. Jafari, E. Assadpoor and D. Dehnad, Microencapsulation optimization of natural anthocyanins with maltodextrin, gum Arabic and gelatin, *Int. J. Biol. Macromol.*, 2016, **85**, 379–385.
- 63 B. Bazaria and P. Kumar, Effect of whey protein concentrate as drying aid and drying parameters on physicochemical and functional properties of spray dried beetroot juice concentrate, *Food Biosci.*, 2016, **14**, 21–27.

